Subspace-based Blind Multi-user Detection for TH-UWB Systems in Multi-path Channels

Chia-Hsin Cheng [1], Wen-Jun Lin [2], Kai-Jie Chen [3]
[1, 3]The Department of Computer and Communication Engineering
Chaoyang University of Technology, Taiwan
[2]The Institute of Communication Engineering
National Chung Cheng University, Taiwan
e-mail: chcheng@cyut.edu.tw

Abstract: - A subspace-based blind adaptive linear minimum mean square error (MMSE) detector has been proposed for multi-user detection in a direct sequence code-division multiple-access (CDMA) system even when multi-path channels are unknown. In this paper, the applicability of the subspace-based blind adaptive algorithm in multiple access ultra-wideband (UWB) systems is investigated. The problem of blind demodulation of multi-user information symbols in a high-rate UWB network in the presence of both multiple access interference (MAI) and inter-symbol interference (ISI) is also considered. Moreover, the Rake receiver is adopted to collect multi-path gains. The performance of the subspace-based blind techniques is shown under time-variant UWB multi-path channels.

Key-Words: - Ultra-wideband, Blind adaptation, Multi-user detection, Subspace tracking.

1 Introduction

Recently, time-hopping ultra wide-band (TH-UWB) communication systems have been widely studied and developed due to their appealing features [1]. UWB systems are promising wireless communication systems which offer high bit rate transmission, and can be used for a wide set of applications [2-7], from wireless local area networks (LANs) to ad hoc networks, from IP mobile-computing to multimedia-centric applications. UWB technology brings the convenience and mobility of wireless communications to high-speed interconnections in devices throughout the digital home and office.

In the design and analysis of low-rate systems, the presence of inter-symbol interference (ISI) due to the multi-path nature of wireless channels is often neglected [8]. However, for high-rate UWB systems, ISI is not negligible and, in fact, together with multiple-access interference (MAI) which is inherent in non-orthogonal UWB systems. As with high speed direct sequence-code division multiple access (DS-CDMA) systems, these two major impediments (ISI and MAI) cause a receiver to be incapable of completely removing the presence of undesired signals, which eventually results in large performance degradation.

Over the past decade, a significant amount of research has addressed various multi-user detection schemes [9]. Since, in a dynamic environment, it is very difficult for a mobile user to obtain accurate information on other active users in a channel; several papers have focused on blind multi-user detection [10-15]. These blind techniques essentially allow a given user to use a linear multi-user detector with no knowledge beyond that required for implementing a conventional detector for that user. Moreover, blind channel estimation algorithms techniques have been proposed [16-19] to get channel state information.

In this paper, we are going to extend the subspace-based blind linear MMSE detector in [8] to the TH-UWB system, and use the proposed projection approximation subspace-tracking (PASTd) algorithm [20] for the blind adaptive multi-user detection application. Based on several typical UWB channels according to the IEEE proposed UWB channel model [25, 26], a Rake receiver is adopted to mitigate multi-path distortion. The Rake receiver resolves the components of a received signal (arriving at different times) and combines them to provide diversity. A comparison of the performance between the equal gain combing (EGC) and the maximal ratio combining (MRC) schemes are given in this paper. We investigate the performance of the subspace-based blind multi-user detection for the TH-UWB communication systems in UWB channels.

The rest of this paper is organized as follows. In Section 2, the TH-UWB system model is presented. In Section 3, we describe the subspace-based blind adaptive linear MMSE multi-user detector. In Section 4, simulation examples are provided in four

types of the IEEE proposed channel mode. Finally, the conclusions appear in Section 5.

2 System Model

In the TH-UWB system, the transmitted signal $s_{tx}^{(k)}(t)$ for user k using a binary phase-shift keyed (BPSK) modulation can be defined as [3, 4]

$$s_{tx}^{(k)}(t)=\sqrt{E_k}\sum_{n=-\infty}^{\infty}b_k(n)\sum_{m=0}^{N_f-1}d_k(m)w_{tx}(t-nT_s-mT_f-c_m^{(k)}T_c) \quad (1)$$

where $w_{tx}(t)$ represents the transmitted monocycle pulse waveform with unit energy, E_k is the transmitted energy per symbol for user k, T_f and T_c are the average pulse repetition period and the chip duration of the TH code, respectively, N_f is the number of pulses representing one information symbol of length T_s, and $b_k \in \{+1,-1\}$ is the information symbol transmitted by user k. A pseudo-random time-hopping code $\{c_m^{(k)}\}$, $c_m^{(k)} \in \{0, 1, ..., N_c-1\}$, $\forall k$, provides an additional shift of $c_m^{(k)}T_c$ seconds in order to avoid catastrophic collisions in multiple access channels. T_c is chosen to satisfy $T_c \le T_f/N_c$ to prevent interpulse interference (IPI). Without loss of generality, $T_f = N_cT_c$ is assumed throughout this paper. Random polarity codes $d_k(m)$ are binary random variables taking values $\{\pm 1\}$ with equal probability, and $d_k(m)$ and $d_q(p)$ are independent for $(k,m)\neq(q,p)$ .Please, leave two blank lines between successive sections as here.

With a modification of the definition proposed by E. Fishler and H. V. Poor [3], we define a sequence $\{s_k(m)\}$ as follows:

$$s_k(m)=\begin{cases} d_k(\lfloor m/N_c\rfloor) & , \quad m-N_c(\lfloor m/N_c\rfloor)=c_{\lfloor m/N_c\rfloor}^{(k)} \\ 0 & , \quad \text{otherwise} \end{cases} \quad (2)$$

where $\lfloor\cdot\rfloor$ denotes the integer part.

The transmitted signal of user k can be rewritten as follows:

$$s_{tx}^{(k)}(t)=\sqrt{E_k}\sum_{n=-\infty}^{\infty}b_k(n)\sum_{m=0}^{N-1}s_k(m)w_{tx}(t-nT_s-mT_c) \quad (3)$$

where $N \equiv N_fN_c$. Then, a TH-UWB with polarity randomization can be regarded as a random CDMA (RCDMA) system with a generalized spreading sequence $\{s_k[m]\}$, where the elements of the sequence take values from $\{-1, 0, +1\}$.

A UWB channel model can be modeled as a discrete linear filter with an impulse response [26]. We consider transmission over a frequency selective channel. The impulse response for user k can be modeled as:

$$h_k(t)=\sum_{l=1}^{L_k}\tilde{h}_{k,l}\delta(t-(l-1)T_c) \quad (4)$$

where $\tilde{h}_{k,l}$ and L_k are the channel coefficient of the lth path and the number of paths of user k, respectively. $\delta(\cdot)$ is the Dirac delta function. To simplify analysis, we assume T_c is the minimum path resolution and is equal to the pulse duration for the proposed UWB system. Multi-path arrivals are assumed to be at integral multiples of the minimum resolution time.

For analysis, it is assumed throughout the rest of this paper that the system considered is a synchronous system. An asynchronous system of K users can then be viewed as equivalent to a synchronous system with $2K-1$ users [23]. The received signal $r(t)$ can be expressed as follows:

$$r(t)=\sum_{k=1}^{K}\sqrt{E_k}\sum_{n=-\infty}^{\infty}b_k(n)\sum_{m=0}^{N-1}\sum_{l=1}^{L_k}\tilde{h}_{k,l}s_k(m) \times w_{rx}(t-nT_s-mT_c-(l-1)T_c)+v(t) \quad (5)$$

where $v(t)$ is a zero mean white Gaussian noise process with variance σ^2, and $w_{rx}(t)$ is a received UWB pulse with unit energy.

3 Subspace-Based Detection

In this section, we adopt a subspace approach to blind multi-user detection which was first proposed by Wang and Poor [10] and which is based on estimating the signal subspace spanned by the user signature waveforms. At the receiver, the received signal $r(t)$ is passed through a linear filter matched to the received pulse $w_{rx}(t)$, and then is sampled at the chip rate. The *j*th chip of the *i*th symbol is represented as

$$\begin{aligned} z_i[j] &= z(t)\big|_{t=iT_s+jT_c} \\ &= \sum_{k=1}^{K}\sqrt{E_k}\sum_{n=-\infty}^{\infty}b_k(n)\sum_{m=0}^{N-1}s_k(m)\sum_{l=1}^{L_k}\tilde{h}_{k,l}\delta((i-n)T_s+(j-m)T_c-(l-1)T_c) \\ &\quad +\tilde{v}[iT_s+jT_c] \end{aligned} \quad (6)$$

In a realistic UWB environment, the received signal will suffer ISI because of a lot of multi-path channels. Without loss of generality, assume user 1 is the desired user. Fig. 1 shows the structure of the Rake receiver for user 1. The vector form of the output of the chip matched filter for the *i*th symbol of the *l*th finger of the Rake receiver is

$$\mathbf{y}_l[i]=\begin{bmatrix} z_i[l] & z_i[l+1] & \cdots & z_i[N+l-1]\end{bmatrix}^T_{(N\times 1)} \quad (7)$$

In this paper, we assume that the maximum delay spread is within one symbol duration. Each finger of the Rake receiver is assumed to be a regular delay at integral multiples of the minimum resolution time Tc. Hence, for the *l*th finger, (7) can be reformulated in the following matrix form:

$$\mathbf{y}_l[i]=\sqrt{E_1}b_1(i)\tilde{\mathbf{s}}_{1,l}\mathbf{h}_1+ISI+MAI+\mathbf{v}_l[i] \quad (8)$$

where

$$ISI=\sqrt{E_1}b_1(i-1)\tilde{\mathbf{s}}^-_{1,l}\mathbf{h}_1+\sqrt{E_1}b_1(i+1)\tilde{\mathbf{s}}^+_{1,l}\mathbf{h}_1$$

$$MAI=\sum_{k=2}^{K}\sqrt{E_k}b_k(i-1)\tilde{\mathbf{s}}^-_{k,l}\mathbf{h}_k+\sqrt{E_k}b_k(i)\tilde{\mathbf{s}}_{k,l}\mathbf{h}_k+\sqrt{E_k}b_k(i+1)\tilde{\mathbf{s}}^+_{k,l}\mathbf{h}_k$$

$$AWGN=\mathbf{v}_l[i]$$

$$\tilde{\mathbf{s}}^-_{k,l}=\begin{bmatrix} 0 & \cdots & \cdots & \cdots & \cdots & \cdots & 0\\ \vdots & & & & & & \vdots\\ 0 & & & & & & 0\\ s_k(N-1) & 0 & \cdots & & & \cdots & 0\\ s_k(N-2) & s_k(N-1) & 0 & & \cdots & & 0\\ \vdots & & \ddots & \ddots & & & \vdots\\ s_k(N-L+l) & \cdots & \cdots & s_k(N-1) & 0 & \cdots & 0\end{bmatrix}^T$$

, $l=1,\ldots,L$ ($N\times L$ matrix), L is the maximum of L_k, $k=1,\cdots,K$,

$$\tilde{\mathbf{s}}_{k,l}=\begin{bmatrix} s_k(l-1) & \cdots & s_k(N-1) & 0 & \cdots & 0\\ s_k(l-2) & & \cdots & s_k(N-1) & 0 & \vdots\\ \vdots & & & & \ddots & 0\\ s_k(0) & & & & \cdots & s_k(N-1)\\ 0 & s_k(0) & & & \cdots & s_k(N-2)\\ \vdots & \ddots & & & & \vdots\\ 0 & \cdots & 0 & s_k(0) & \cdots & s_k(N-L+l-1)\end{bmatrix}^T, l=1,\ldots,L$$

($N\times L$ matrix) and

$$\tilde{\mathbf{s}}^+_{k,l}=\begin{bmatrix} 0 & \cdots & 0 & s_k(0) & \cdots & \cdots & s_k(l-2)\\ \vdots & & \vdots & \ddots & \ddots & & \vdots\\ \vdots & & & & 0 & s_k(0) & s_k(1)\\ 0 & & & & \vdots & 0 & s_k(0)\\ \vdots & & & & & \vdots & 0\\ \vdots & & & & & & \vdots\\ 0 & \cdots & \cdots & \cdots & & & 0\end{bmatrix}^T, l=1,\ldots,L$$

($N\times L$ matrix) are the signature. $\mathbf{h}_k=[\tilde{h}_{k,1} \quad \cdots \quad \tilde{h}_{k,L_k}]^T$ ($L\times 1$ vector) is the vector of the channel coefficient for the *k*th user, and $\mathbf{v}_l[i]=[\tilde{v}[l] \quad \tilde{v}[2] \quad \cdots \quad \tilde{v}[N+l-1]]^T$ ($N\times 1$ vector) is the matched filter output noise vector and is a Gaussian noise vector with mean 0 and covariance matrix $\sigma^2\mathbf{I_N}$ ($\mathbf{I_N}$ denotes the $N\times N$ identity matrix).

In (8), the first term contains the *i*th bit of user 1; the second term contains the ISI from the (*i*-1)th and (*i*+1)th bits of user 1; the third term contains the MAI from other users, and the last term is the ambient channel noise.

We can rewrite $\mathbf{y}_l[i]$ in a compact form as follows:

$$\mathbf{y}_l[i]=\underbrace{\tilde{\mathbf{S}}_l^-\mathbf{HA}}_{\tilde{\mathbf{G}}_l^-}\mathbf{b}(i-1)+\underbrace{\tilde{\mathbf{S}}_l\mathbf{HA}}_{\tilde{\mathbf{G}}_l}\mathbf{b}(i)+\underbrace{\tilde{\mathbf{S}}_l^+\mathbf{HA}}_{\tilde{\mathbf{G}}_l^+}\mathbf{b}(i+1)+\mathbf{v}_l[i]$$

$$=\begin{bmatrix}\tilde{\mathbf{G}}_l^- & \tilde{\mathbf{G}}_l & \tilde{\mathbf{G}}_l^+\end{bmatrix}\begin{bmatrix}\mathbf{b}(i-1)\\ \mathbf{b}(i)\\ \mathbf{b}(i+1)\end{bmatrix}+\mathbf{v}_l[i]$$

$$=\mathbf{G}_l\mathbf{B}+\mathbf{v}_l[i] \quad (9)$$

where $\tilde{\mathbf{S}}_l^-=\begin{bmatrix}\tilde{\mathbf{s}}^-_{1,l} & \cdots & \tilde{\mathbf{s}}^-_{K,l}\end{bmatrix}$ ($N\times KL$ matrix),

$\tilde{\mathbf{S}}_l=\begin{bmatrix}\tilde{\mathbf{s}}_{1,l} & \cdots & \tilde{\mathbf{s}}_{K,l}\end{bmatrix}$ ($N\times KL$ matrix),

$\tilde{\mathbf{S}}_l^+=\begin{bmatrix}\tilde{\mathbf{s}}^+_{1,l} & \cdots & \tilde{\mathbf{s}}^+_{K,l}\end{bmatrix}$ ($N\times KL$ matrix),

$\mathbf{H}=diag\{\mathbf{h}_1 \quad \cdots \quad \mathbf{h}_K\}$ ($KL\times K$ matrix),

$\mathbf{A}=diag\{\sqrt{E_1} \quad \cdots \quad \sqrt{E_K}\}$ ($K\times K$ matrix),

$\mathbf{b}(i)=[b_1(i) \quad \cdots \quad b_K(i)]^T$ ($K\times 1$ matrix),

$\mathbf{G}_l=\begin{bmatrix}\tilde{\mathbf{G}}_l^- & \tilde{\mathbf{G}}_l & \tilde{\mathbf{G}}_l^+\end{bmatrix}$ ($N\times 3K$ matrix), and

$\mathbf{B}=[\mathbf{b}(i-1) \quad \mathbf{b}(i) \quad \mathbf{b}(i+1)]^T$ ($3K\times 1$ matrix).

3.1 Subspace Concept

Let $\mathbf{C}_l=\mathrm{E}\{\mathbf{y}_l\,\mathbf{y}_l^T\}$ be the autocorrelation of the received signal of the *l*th finger. We denote its eigendecomposition as

$$\mathbf{C}_l=\mathbf{U}_{s,l}\mathbf{\Lambda}_{s,l}\mathbf{U}^T_{s,l}+\sigma^2\mathbf{U}_{n,l}\mathbf{U}^T_{n,l} \quad (10)$$

where $\mathbf{\Lambda}_{s,l}$=diag$(\lambda_1, \cdots, \lambda_K)$ ($K\times K$ matrix) contains the largest K eigenvalues of $\mathbf{C}_l$ in descending order; $\mathbf{U}_{s,l}=\begin{bmatrix}\mathbf{u}_{1,l} & \cdots & \mathbf{u}_{K,l}\end{bmatrix}$ ($N\times K$ matrix) contains the corresponding orthogonal eigenvectors in $\mathbf{\Lambda}_{s,l}$; and $\mathbf{U}_{n,l}=\begin{bmatrix}\mathbf{u}_{K+1,l} & \cdots & \mathbf{u}_{N,l}\end{bmatrix}$ ($N\times(N-K)$ matrix) contains the (*N*-*K*) orthogonal eigenvectors that correspond to the eigenvalues σ^2 of $\mathbf{C}_l$.

The linear MMSE detector for detecting the 1st user's data bit $b_1(i)$ from the output signal of the *l*th finger is given by [11]

$$\mathbf{w}_{1,l}=\mathbf{U}_{s,l}\mathbf{\Lambda}_{s,l}^{-1}\mathbf{U}^T_{s,l}\mathbf{g}_{1,l} \quad (11)$$

where, for the MRC-Rake case, $\mathbf{g}_{1,l}=\mathbf{G}_l\mathbf{e}_{K+1}=\tilde{\mathbf{s}}_{1,l}\mathbf{h}_1$ and $\mathbf{e}_{K+1}$ is a *3K*-vector with all entries that are zeros except for the *K*+*1*th entry, and for the EGC Rake case, $\mathbf{g}_{1,l}=\tilde{\mathbf{s}}_{1,l}\mathbf{1}_N$ and $\mathbf{1}_N$ is a vector of length *N* with all elements equal to one. We can use blind channel estimation algorithms to get $\mathbf{h}_1$.

After the linear MMSE detector block, the outputs of *L* fingers' signals are combined by a Rake combiner to form user 1 decision variable given by

$$\tilde{b}_1(i)=\sum_{l=1}^{L}\tilde{y}_l[i]=\sum_{l=1}^{L}\mathbf{w}^T_{1,l}\tilde{\mathbf{y}}_l \quad (12)$$

Then, the output of the decision device of the desired user is

$$\hat{b}_1(i) = \mathrm{sgn}(\tilde{b}_1(i)) \tag{13}$$

3.2 Tracking the signal subspace

It was seen from the previous section that linear multi-user detectors are obtained once the signal subspace components are identified. The classic approach to subspace estimation is commonly based on eigenvalue decomposition (EVD) or singular value decomposition (SVD), which is computationally too expensive for adaptive applications. A large number of subspace tracking algorithms have already been introduced [20-22]. For the simulation examples provided in Section 4, we adopt the proposed projection approximation subspace tracking (PASTd) algorithm [20] for the blind adaptive multi-user detection application. The advantages of this algorithm include almost certain global convergence to the signal eigenvectors and eigenvalues and low computational complexity $(O(NK))$.

4 Simulation Results

We adopt the Rake receiver with subspace-based blind linear MMSE detector in UWB channels. The structure of the Rake receiver with equal gain combining (EGC) or maximal ratio combining (MRC) is shown in Fig. 1. Based on Intel UWB channel extensive measurements in an indoor environment, UWB systems appear with four typical channel characteristics in an indoor environment (e.g. channel model 1(CM1), CM2, CM3 and CM4). The model parameters were found by experiment to match different UWB channel characteristics [26]. Some parameters used in this experiment are as follows: $SNR_k = 10\log(E_k/\sigma^2)$ (k = 1, 2, …, K); the number of pulses representing one information symbol is N_f=8 ; the number of chips per frame is N_c=16 ; the number of users is K=6; the desired user is user 1, and all users have the same transmitted energy. The signal-to-noise ratio before spreading is 20 dB. The performance measure is the post-combining signal-to-interference ratio (SIR), defined as

$$\mathrm{SIR} \triangleq \frac{E^2\left\{\sum_{l=1}^{L} \mathbf{w}_{1,l}^T \mathbf{y}_l\right\}}{Var\left\{\sum_{l=1}^{L} \mathbf{w}_{1,l}^T \mathbf{y}_l\right\}} \tag{14}$$

where the expectation is with respect to the data bits of interfering users, the ISI bits, and the ambient noise. The SIR is a particularly useful figure of merit for MMSE detectors since it has been shown [24] that the output of an MMSE detector is approximately Gaussian distributed. Hence, the SIR values translate directly and simply to bit-error probabilities.

In the simulation, the expectation operation is replaced by the time averaging operation. The PASTd algorithm is used for updating the signal subspace components at every time step to produce the approximate SVD. For the PASTd subspace tracking algorithm, we found that with a random initialization, the convergence is fairly slow. Therefore, in the simulations, the initial estimates of the eigencomponents of the signal subspace are obtained by applying an SVD to the first 50 data vectors [10]. The forgetting factor used in the PASTd algorithm is 0.995. The time-averaged outputs SIR with EGC and MRC diversity techniques versus the number of iterations in four types of channel models are plotted in Figs. 2-5. The number of Rake's fingers for each channel model is selected by the receiver, which can capture 95% of the total received energy. As expected, it can be seen that the performance of MRC is better than that of EGC. In Fig. 5, compared with the simulation results for CM1, CM2, and CM3, the simulation result for CM4 (extreme NLOS environment) indicates that the system performance is severely affected by multi-path interference.

Figs. 6-10 show the subspace-based blind adaptive multi-user detector with MRC-Rake over a time-varying channel. In the simulation, the environment of the receiver is suddenly changed at $t = 2001$. Figs. 6-10 indicate different SIRs in different dynamic environments, i.e., i.e., CM1 to CM4, CM4 to CM1, CM1 to CM1 (different channel coefficients), CM1 to CM2 and CM1 to CM3. In Fig. 11, the environment of the receiver is suddenly changed at t = 2001, 4000, and 6001. From these figures, it can be seen that this subspace-based blind adaptive multi-user detector can adapt well to the time-varying channel environment. The performance, good or bad, mainly depends on which channel model the system uses.

5 Conclusion

In this paper, using the subspace-based concept, we proposed a subspace-based blind adaptive linear MMSE multi-user detector in TH-UWB systems. In the receiver, we adopt the Rake combiner structure to provide diversity gain from multi-path channels. The performance comparison of the MRC and EGC Rake receiver are presented in four types of UWB channel models proposed by the IEEE standards body. Moreover, the simulation results show the subspace-based blind algorithm combined with the Rake technique can be used effectively for reducing the effects of ISI and MAI. It adapts well to a time-varying UWB multi-path channel.

References:

[1] M. Z. Win, R. A. Scholtz, "Ultra-wide bandwidth time-hopping spread-spectrum impulse radio for wireless multiple-access communications," *IEEE Trans. Commun.*, Vol. 48, No.4, pp. 679-691, Apr. 2000.

[2] F. Cuomo, C. Martello, A. Baiocchi, F. Capriotti, "Radio resource sharing for ad-hoc networking with UWB," *IEEE J. Select. Areas Commun.*, Vol. 20, No. 9, pp. 1722-1732, Dec. 2002.

[3] E. Fishler and H. V. Poor, "On the tradeoff between two types of processing gains," *IEEE Trans. Commun*. Vol. 53, pp. 1744-1753, 2005.

[4] S. Gezici, H. Kobayashi and H. V. Poor, "A comparative study of pulse combining schemes for impulse radio UWB systems," *Proc. IEEE Sarnoff Symposium 2004,* pp. 7-10, Princeton, NJ, Apr.l 26-27, 2004.

[5] T. Erseghe, "Time-Hopping Patterns derived from Permutation Sequences for UWB-IR Applications," *Proc. of 6th WSEAS Int. Conf. on Commum.*, no. 1, Vol. 1, pp. 109-115, Crete, July 7-14, 2002.

[6] Shing TenqChen, Ying-Haw Shu, Ming-Chang Sun, Wu-Shiung Feng and Chao-Hao Lee, "Performance comparison of PPM-TH, PAM-TH, and PAM-DS UWB rake receivers with channel estimators via correlation mask," *WSEAS Trans. Commum.*, No 9, Vol. 4, pp. 751-756, September 2005.

[7] Tan-Hsu Tan, Yun-Chung Shen, and Yung-Fa Huang, "Performance Analysis of Multi-User DS-UWB System under Multipath Effects," in *Proc.of the 12th WSEAS Int. Conf. on Commum.*, pp. 117-122, Heraklion, Greece, July 23-25, 2008.

[25] J. G. Proakis, *Digital Communication*, 4th ed., McGraw-Hill, New York, 2001.

[26] S. Verdu, *Multiuser Detection*, Cambridge, U.K.: Cambridge Univ. Press, 1998.

[10] X. Wang and H. V. Poor, "Blind multiuser detection: a subspace approach," *IEEE Trans. Inform. Theory*, Vol. 44, pp. 677-690, March 1998.

[11] X. Wang, and H. V. Poor, "Blind equalization and multiuser detection in dispersive CDMA channels," *IEEE Trans. Commun.*, Vol. 46, No. 1, pp. 91-103, Jan. 1998.

[12] M. Honig, U. Madhow, and S. Verdú, "Verdu, S.: Blind adaptive multiuser detection," *IEEE Trans. Inform. Theory*, Vol. 41, No. 4, pp. 944-960, July 1995.

[13] Z. Xu, P. Liu, and X. Wang, "Blind multiuser detection: from MOE to subspace methods," *IEEE Trans. Signal Process.*, Vol. 52, No. 2, pp.510-524, Feb. 2004.

[14] J. H. Wen and C. K. Wen, "Adaptive recursive algorithm for complementary subspace based blind multiuser detection," *IEEE Trans. Circuits and Systems II: Analog and Digital Signal Processing*, Vol. 48, pp. 1132-1136. Dec. 2001.

[15] S. Buzzi, M. Lops, and H. V. Poor, "Blind adaptive joint multiuser detection and equalization in dispersive differentially encoded CDMA channels," *IEEE Trans. Signal Processing*, Vol. 51, pp. 1880 - 1893, July 2003.

[16] X. G. Doukopoulos and G. V. Moustakides, "Adaptive power techniques for blind channel estimation in CDMA systems," *IEEE Trans. Signal Process.*, Vol.53, No. 3, pp. 1110-1120, March 2005.

[17] Z. Xu and M. K. Tsatsanis, "Blind adaptive algorithms for minimum variance CDMA receivers," *IEEE Trans. Commum.*, Vol. 49, o. 1, pp.180-194, Jan. 2001.

[18] H. liu and G. Xu, "A subspace method for signature waveform estimation in synchronous CDMA systems," *IEEE Trans. Commun.*, Vol. 44, pp. 1346–1354, Oct. 1996.

[19] S. E. Bensley and B. Aazhang, "Subspace-based channel estimation for code division multiple access communication systems," *IEEE Trans. Commun.*, Vol. 44, pp. 1009–1020, Aug. 1996.

[20] B. Yang, "Projection approximation subspace tracking" *IEEE Trans. Signal Process.*, Vol. 43, No.1, pp. 95-107, Jan. 1995.

[21] P. Strobach, "Bi-iteration SVD subspace tracking algorithms," *IEEE Trans. Signal Process*., Vol. 45, No. 5, pp. 1222-1240, May, 1997.

[22] Y. Miao and Y. Hua, "Fast subspace tracking and neural network learning by a novel information criterion," *IEEE Trans. Signal Process.*, Vol. 46, No. 7, pp. 1967-1979, Jul. 1998.

[23] U. Madhow and M. Honig, "MMSE interference suppression for direct-sequence spread-spectrum CDMA," *IEEE Trans. Commun*., Vol. 42, pp. 3178-3188, Dec. 1994.

[24] H. V. Poor and S. Verdu, "Probability of error in MMSE multiuser detection," *IEEE Trans. Inform. Theory*, Vol. 43, pp. 868-971, May 1997.

[25] J. Foerster et al., "Channel modeling sub-committee report final," IEEE 802. 15 Working Group for Wireless Personal Area

Networks (WPANs), IEEE P802.15-02/490r1 -SG3a, Feb. 2003.

[26] A. F. Molisch, J. R. Foerster, and M. Pendergrass, "Pendergrass,M.: Channel models for ultrawideband personal area networks," *IEEE Personal Commun. Mag.*, Vol. 10, No. 6, pp. 14-21, Dec. 2003.

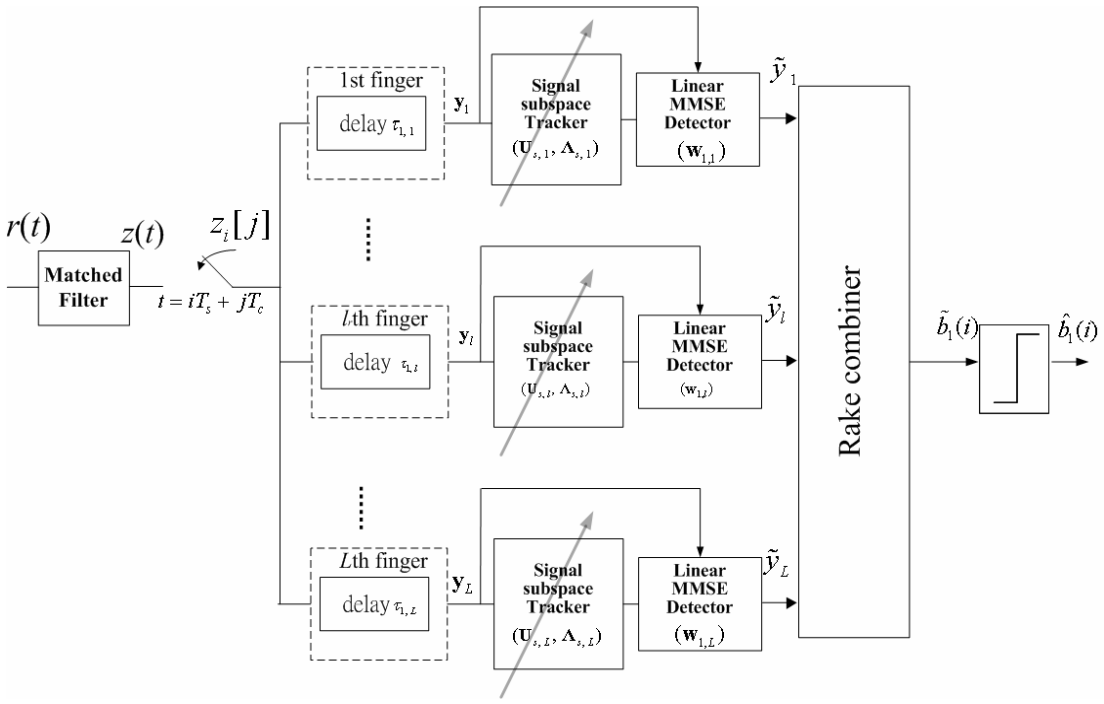

Fig. 1. The Rake receiver structure for subspace-based blind adaptive linear MMSE multi-user detector

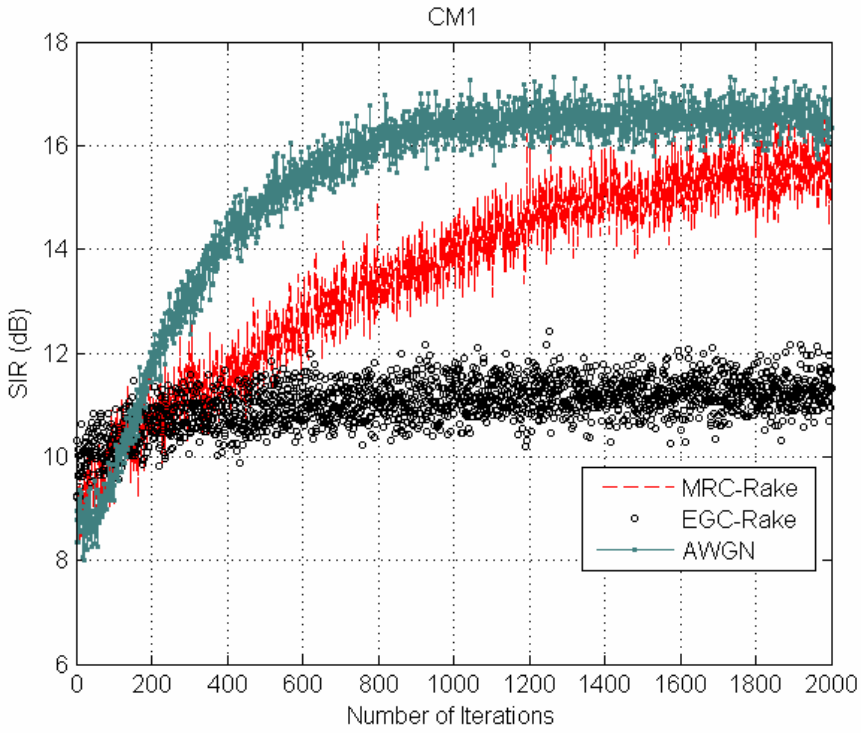

Fig. 2. Performance comparison of the subspace-based blind MMSE detector with EGC-Rake and MRC-Rake in CM1. The data plotted is the average over 200 independent runs**.**

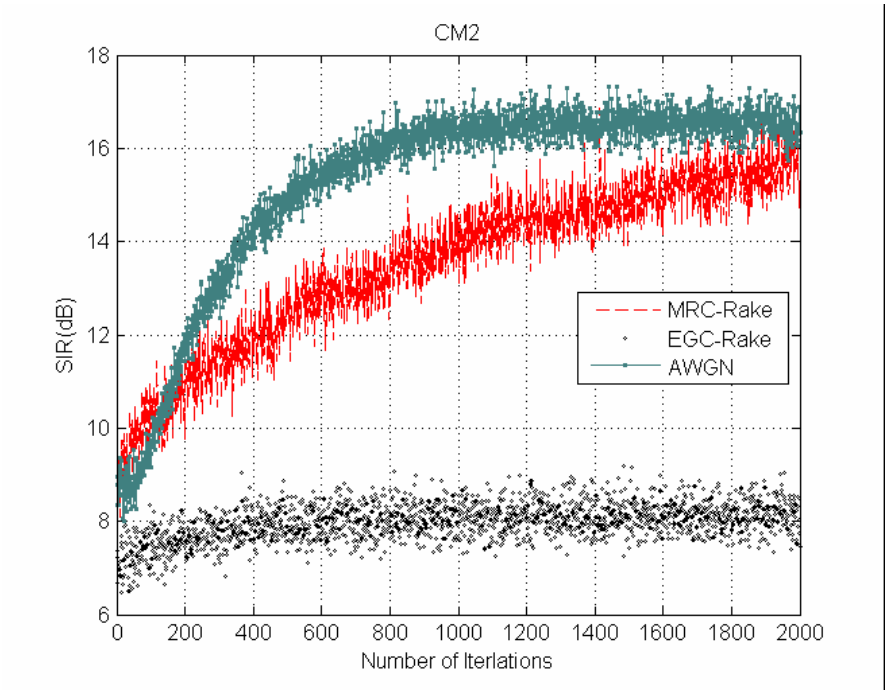

Fig. 3. Performance comparison of the subspace-based blind MMSE detector with EGC-Rake and MRC-Rake in CM2. The data plotted is the average over 200 independent runs.

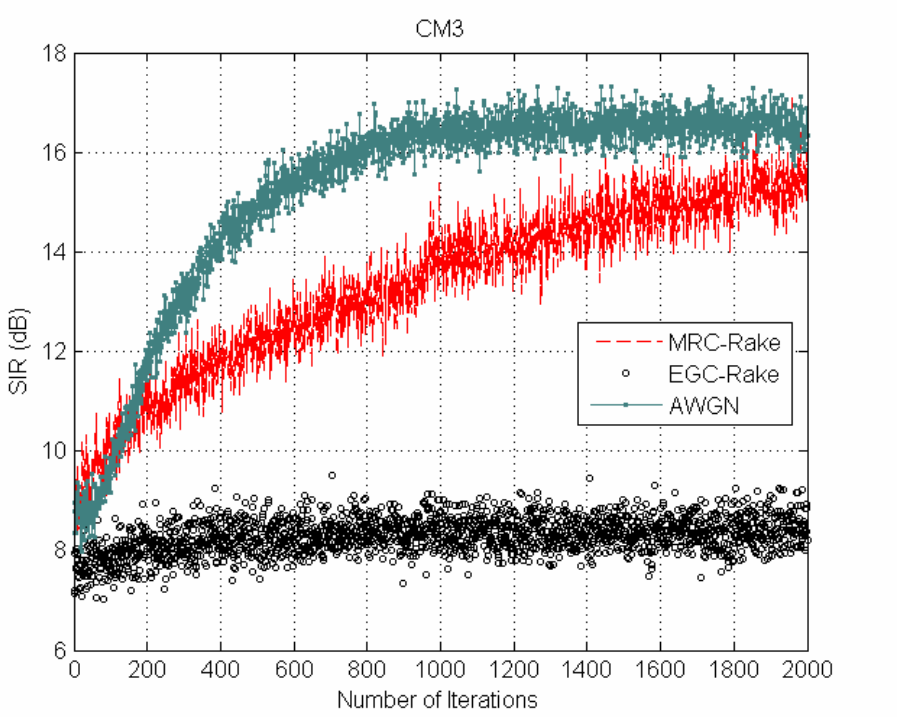

Fig. 4. Performance comparison of the subspace-based blind MMSE detector with EGC-Rake and MRC-Rake in CM3. The data plotted is the average over 200 independent runs.

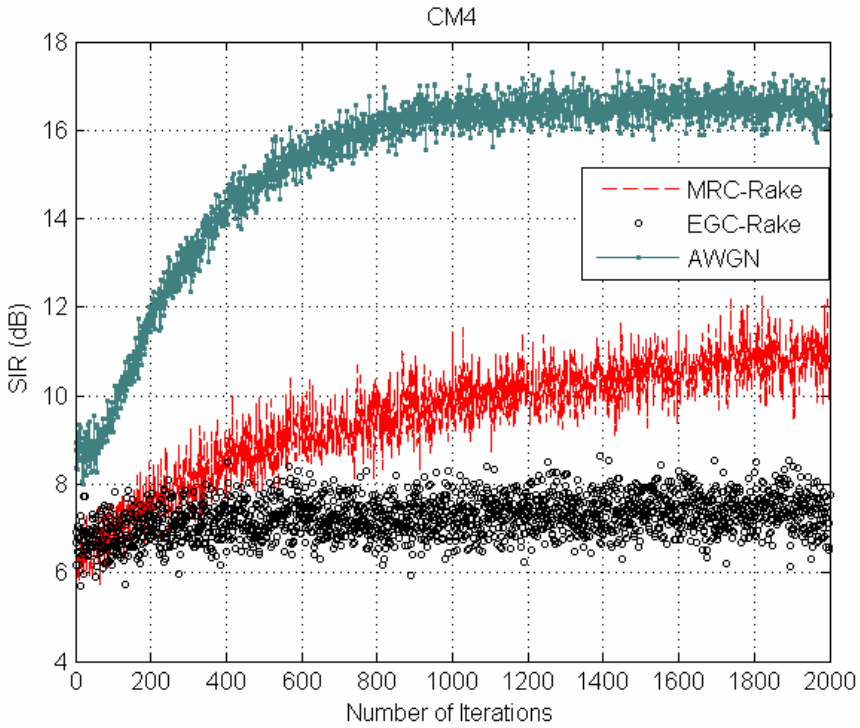

Fig. 5. Performance comparison of the subspace-based blind MMSE detector with EGC-Rake and MRC-Rake in CM4. The data plotted is the average over 200 independent runs.

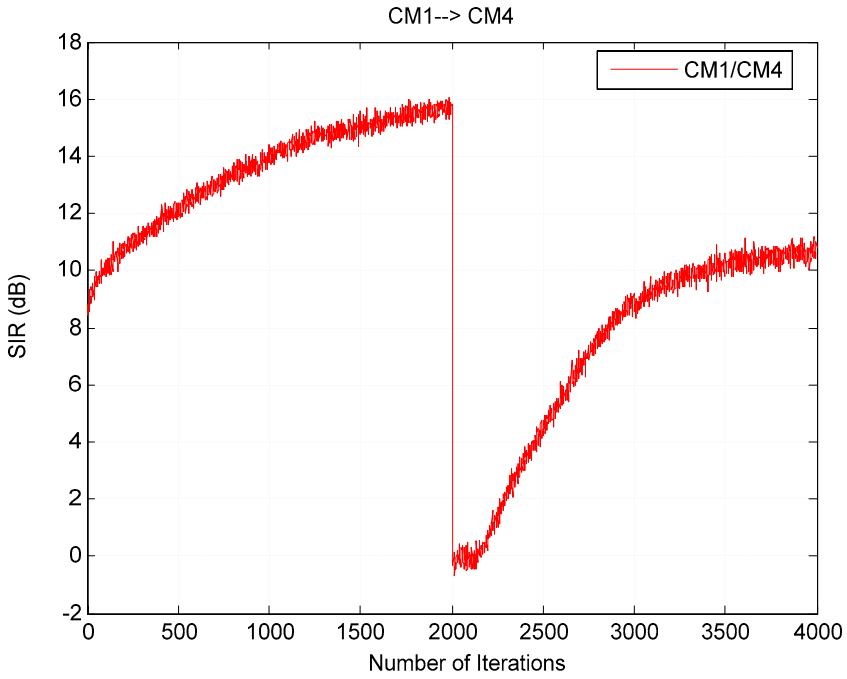

Fig. 6. Performance of the subspace-based blind linear MMSE detector with MRC-Rake over a time-varying channel environment. The simulation starts ($t = 0$) in the CM1 channel; at $t = 2001$, in the CM4 channel. The data plotted is the average over 500 runs.

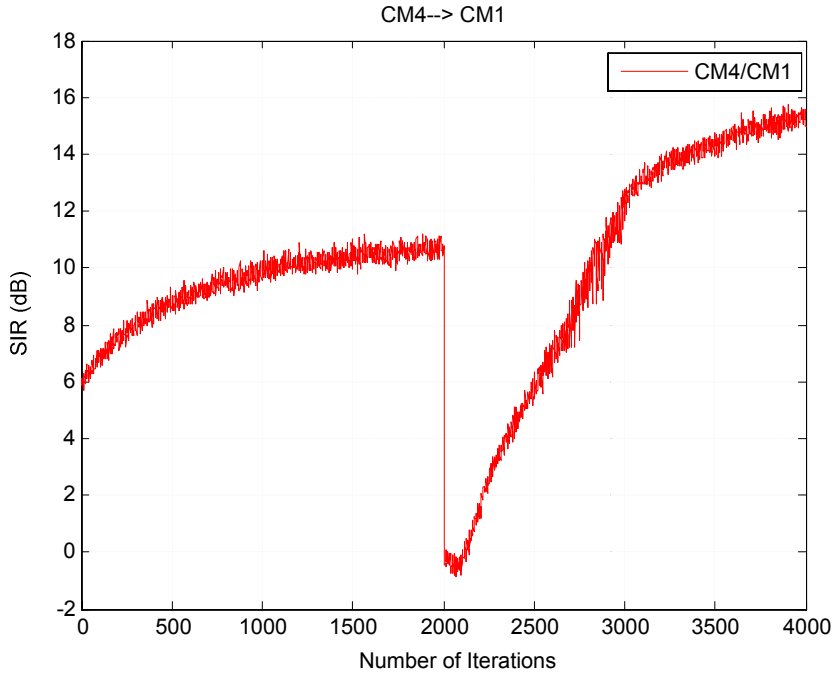

Fig. 7. Performance of the subspace-based blind linear MMSE detector with MRC-Rake over a time-varying channel environment. The simulation starts ($t = 0$) in the CM4 channel; at $t = 2001$, in the CM1 channel. The data plotted is the average over 500 runs.

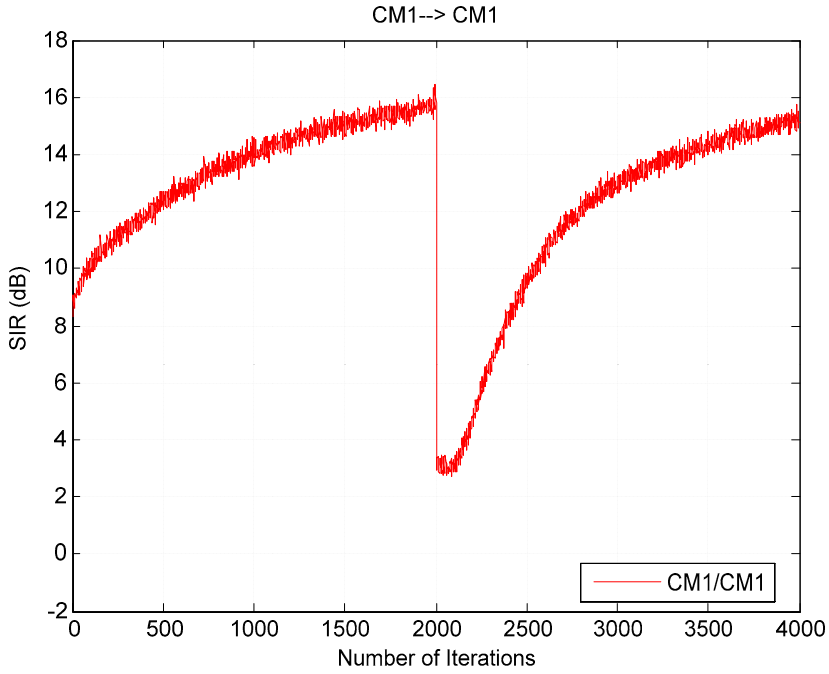

Fig. 8. Performance of the subspace-based blind linear MMSE detector with MRC-Rake over a time-varying channel environment. The simulation starts ($t = 0$) in the CM1 channel; at $t = 2001$, in another CM1 channel (different channel coefficients). The data plotted is the average over 500 runs.

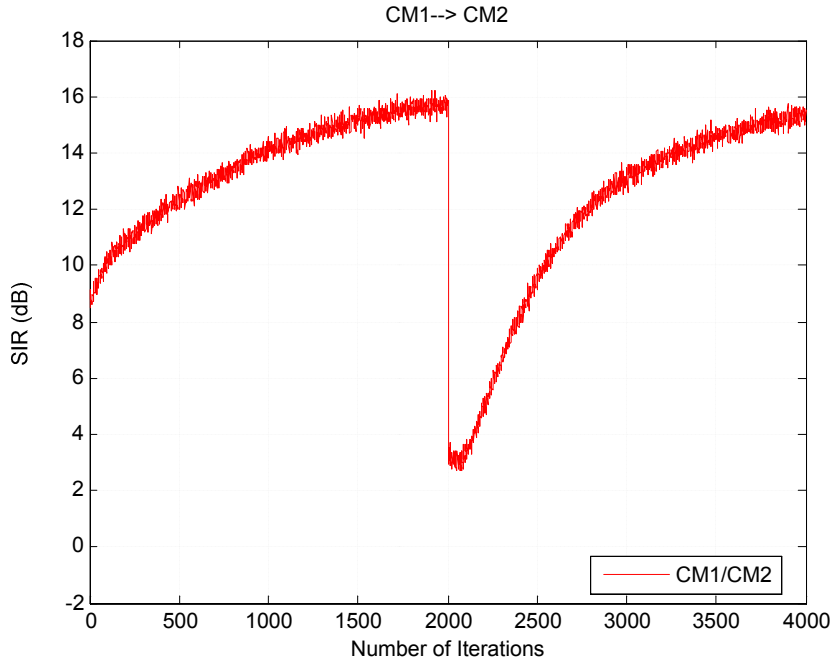

Fig. 9. Performance of the subspace-based blind linear MMSE detector with MRC-Rake over a time-varying channel environment. The simulation starts ($t = 0$) in the CM1 channel; at $t = 2001$, in the CM2 channel. The data plotted is the average over 500 runs.

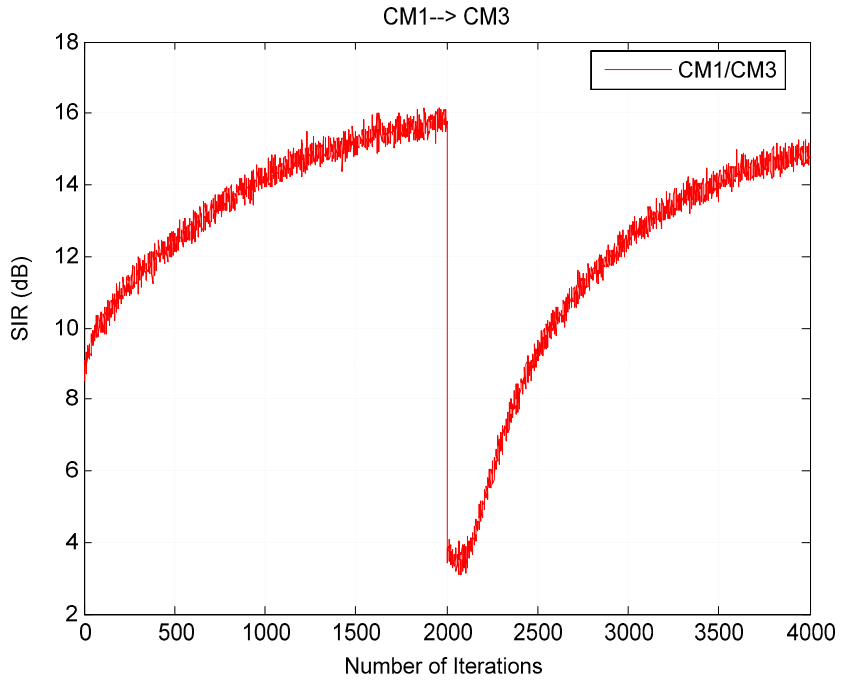

Fig. 10. Performance of the subspace-based blind linear MMSE detector with MRC-Rake over a time-varying channel environment. The simulation starts ($t = 0$) in the CM1 channel; at $t = 2001$, in the CM3 channel. The data plotted is the average over 500 runs.

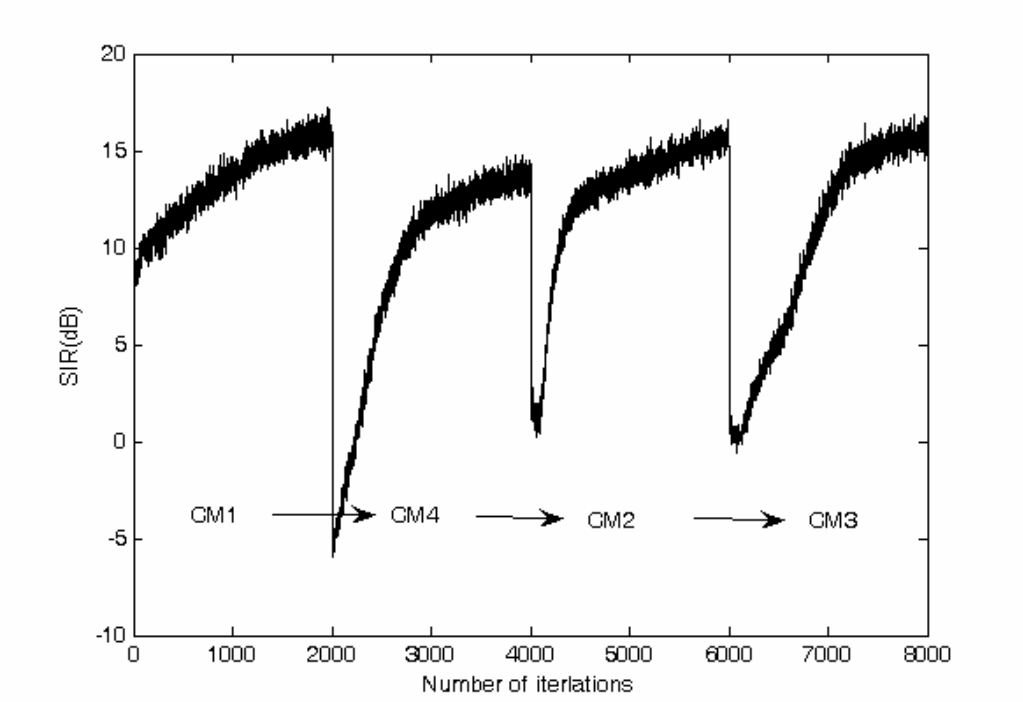

Fig. 11. Performance of the subspace-based MRC-Rake receiver over a time-varying channel. The simulation starts ($t = 0$~2000) in CM1; at $t = 2001$~4000 in CM4; at $t = 4001$~6000 in CM2; at $t = 6001$~8000 in CM3. The data plotted are the average over 500 simulations.